PERGAMON

Journal of Structural Geology 23 (2001) 223–238

JOURNAL OF STRUCTURAL GEOLOGY

www.elsevier.nl/locate/jstrugeo

Fracture termination and step-over at bedding interfaces due to frictional slip and interface opening

Michele L. Cooke[a,*], Chad A. Underwood[b,1]

[a]Geosciences Department, University of Massachusetts—Amherst, Amherst, MA 01003, USA
[b]Geological Engineering Program, University of Wisconsin—Madison, Madison, Wisconsin, USA

Received 18 January 2000; accepted 26 June 2000

Abstract

Three types of fracture intersection with bedding contacts have been investigated within numerical experiments: fracture transection through bed contacts, termination (abutment) at contacts and step-over of fractures at bedding contacts. To evaluate the mechanisms responsible for different fracture intersections with bed contacts, the numerical experiments explored deformation associated with end-member conditions of sliding-only interfaces and opening-only interfaces. A third suite of models explored the combined influence of both sliding and opening, as a fracture approached the interface. In contrast to our initial supposition that interface sliding promotes fracture termination, the sliding-only interfaces encouraged propagation of fractures straight through the modeled interface. In contrast, the opening-only interfaces yielded either fracture termination or initiation of a new fracture near the ends of the open interface segment (several centimeters from parent fracture in these models). These results suggest that local interface opening near the tip of approaching fractures, rather than sliding, is responsible for fracture termination and step-over at bedding contacts. Combined sliding and opening yielded fracture termination in models with weak interfaces ($\mu = 0$; $c = 0$ MPa; $T = 0$ MPa) and either fracture step-over or termination at moderate-strength interfaces ($\mu = 0.65$; $c = 3.25$ MPa; $T = 5$ MPa). Fracture termination occurs at moderate-strength interfaces when the stresses along the interface are not great enough to initiate a new step-over fracture. Fracture termination is more likely under conditions of shallower burial depth, lower layer-parallel effective tension and fluid-driven fracture propagation rather than remote layer-parallel tension. Furthermore, thicker beds and greater layer-parallel effective tension may produce greater distances of fracture step-over than thinner beds and more compressive layers. These results may assist in the prediction of subsurface fracture networks and associated fluid flow paths.

1. Introduction

In layered sedimentary rocks, opening-mode fractures have been observed to abut against bedding contacts (Baer, 1991; Narr and Suppe, 1991; Gross et al., 1995; Becker and Gross, 1996; Ji and Saruwatari, 1998; Underwood, 1999) cross through contacts (e.g. Becker and Gross, 1996), and jog or step-over at bedding contacts (Helgeson and Aydin, 1991). Because fluids within low matrix-permeability rocks flow primarily through available fracture networks (e.g. Nelson, 1985), we can better predict fluid flow paths if we understand the processes that control the type of fracture intersection with bedding contacts. Within layered sedimentary rocks, the termination of fractures at frequent bedding contacts can limit vertical flow and produce highly tortuous flow paths (e.g. Tsang, 1984). In contrast, fractures that propagate straight-through bedding contacts provide well-connected pathways for vertical fluid flow. A potential intermediate case for fluid flow is a fracture that jogs or steps over a few centimeters at bedding contacts (Helgeson and Aydin, 1991). Composite joints, such those as sketched in Fig. 1, are believed to form by repeated step-over of a propagating fracture across successive bedding contacts (Helgeson and Aydin, 1991).

Although these three types of fracture intersection with bedding are readily recognized in the field (Baer, 1991; Helgeson and Aydin, 1991; Narr and Suppe, 1991; Gross et al., 1995; Becker and Gross, 1996; Ji and Saruwatari, 1998; Underwood, 1999), the mechanisms that control the development of one over the other are not yet well understood. Insight into the controlling mechanisms and parameters would aid the prediction of subsurface fracture networks and subsequent fluid flow paths. This study investigates different modes of bedding contact deformation to

* Corresponding author. Tel.: 00-1-413-577-3142; fax: 00-1-413-545-1200.
E-mail address: cooke@geo.umass.edu (M.L. Cooke).
[1] Present address: Montgomery-Watson, 1 Science Court, Madison, WI 53711, USA.

0191-8141/01/$ - see front matter
PII: S0191-8141(00)00092-4

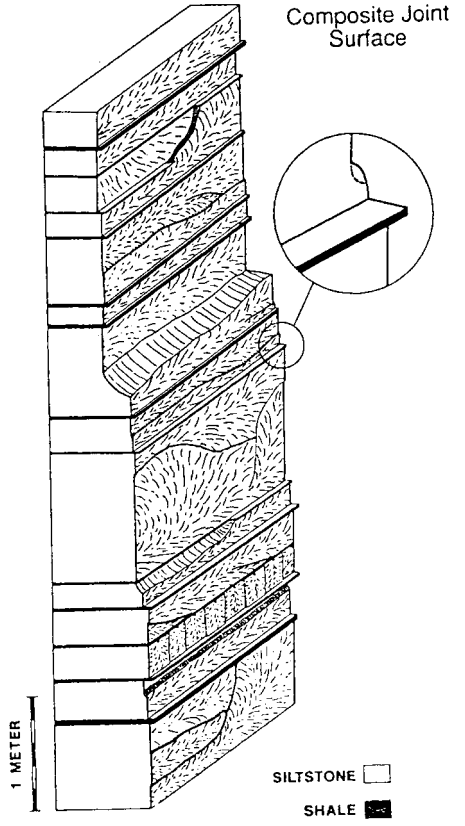

Fig. 1. Sketch of composite joint within interbedded shale and sandstone sequence in New York state. The overall vertical joint trace has a discontinuous nature. Taken from Helgeson and Aydin (1991).

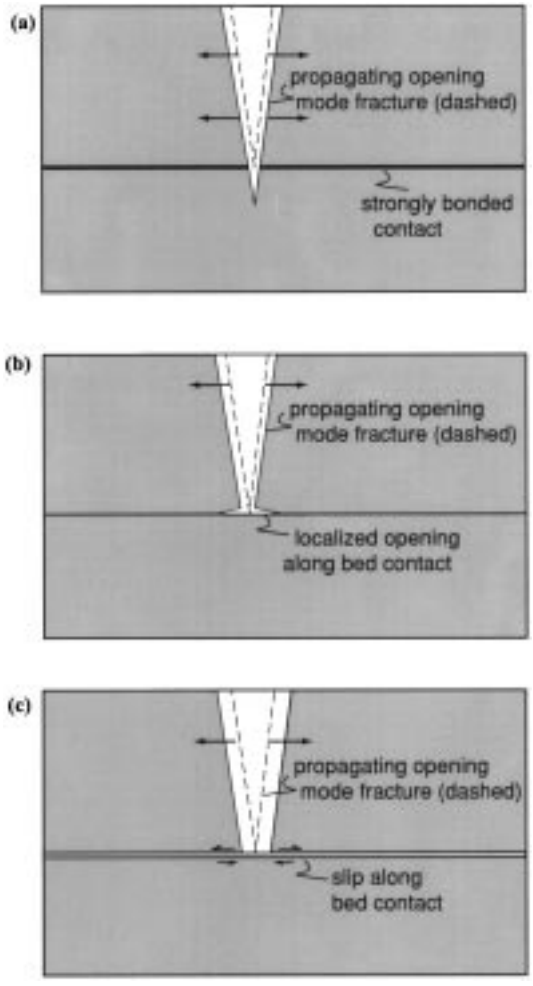

Fig. 2. Postulated mechanisms for fracture propagation through and termination at bedding contacts. (a) Fracture propagation through a strong well-bonded contact within a homogeneous material. (b) Fracture termination at a weakly bonded bedding contact due to local opening of the contact. (c) Fracture termination at a bedding contact due to slip along the contact.

better understand the parameters that control the fracture termination at, propagation through or step-over at bedding contacts.

1.1. Previous work on fracture termination

Previously, field investigations have largely focused on fracture termination in strata consisting of interbedded brittle and ductile rocks (Corbett et al., 1987; Baer, 1991; Helgeson and Aydin, 1991; Narr and Suppe, 1991; Gross et al., 1995; Becker and Gross, 1996; Hanks et al., 1997; Ji and Saruwatari, 1998). In such situations, fractures initiate within stiffer beds (e.g. sandstone, limestone or dolomite) and terminate at the contact with more ductile beds, such as shales and marls (Baer, 1991; Narr and Suppe, 1991; Becker and Gross, 1996; Hanks et al., 1997). Within formations of interbedded brittle and ductile units, two material properties have been demonstrated to govern the propagation of fractures: the stiffness contrast between layers (Cook and Erdogan, 1972; Erdogan and Biricikoglu, 1973; Helgeson and Aydin, 1991) and the yield strength of the more ductile units. In these studies, the contact between layers was perfectly bonded (Fig. 2a).

Only a few field studies (Dyer, 1988; Baer, 1991; Helgeson and Aydin, 1991; Narr and Suppe, 1991; Gross, 1993; Underwood, 1999) discuss the importance of weak bedding contacts on fracture termination. Dyer (1988) and Gross (1993) documented the frequent abutting of cross-joints against older joints. The older joints are inferred to deform by opening and slip during cross-joint development, which influences the propagation of cross-joints towards the older joints (Dyer, 1988; Bai and Gross, 1999). Baer (1991) observed that some dike segments terminate at bedding planes within the dolomite, rather than propagating to shale contacts. These terminations were attributed to bedding-plane slip along the bed contacts (Baer, 1991). Furthermore, Baer (1991) suggested that such dike termination only occurs when the bedding normal stress or friction is extremely low (e.g. at shallow depths). Narr and Suppe (1991) observed, within interbedded dolostone, chert and mudstone/shale, that in addition to fracture termination at mudstone layers, some fractures terminate at mechanical layer boundaries with slickensides, which are indicative of

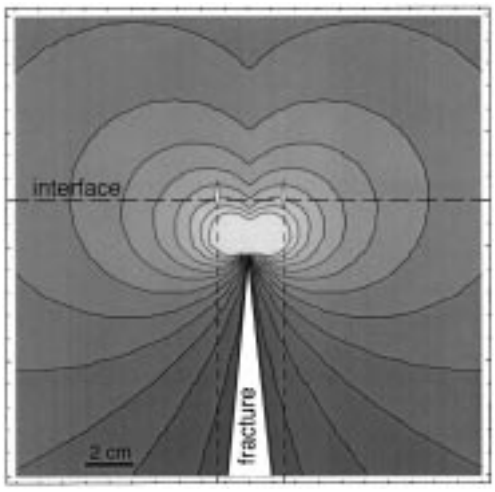

Fig. 3. Maximum tension (principal stress) around the tip of a 1-m vertical fracture under 5-MPa remote isotropic tension. Contours range from 2 to 24 MPa (tension is positive). Along a bonded interface 2 cm ahead of the fracture, the greatest value of maximum tension occurs about 1.5 cm to either side of the parent fracture. Two hypothetical daughter fractures are sketched perpendicular to the maximum tension in these locations ahead of the parent fracture tip.

interlayer slip. Also, Underwood (1999) documented that, within dolostone, fractures terminate at both thin mud layers and weak interfaces, such as thin organic partings and shallowing-upward cycle boundaries.

Most of our present mechanical understanding of the effects of weak mechanical interfaces on fracture development comes from theoretical and laboratory work on Plexiglas™ (Biot et al., 1983), composite materials (e.g. Budiansky and Hutchinson, 1986) and rocks (Weertman, 1980; Teufel and Clark, 1984; Theircelin et al., 1987; Renshaw and Pollard, 1995). An interface that has a low tensile strength is expected to fail by debonding and subsequently to open in the presence of the fracture tip stress field (Fig. 2b). It is postulated that, when the interface opens as the fracture intersects it, the stress singularity at the fracture tip is lost and the fracture may not propagate across the interface. Additionally, a fracture may terminate against a sliding interface when the shear stress at the interface exceeds its shear strength so that the interface slips (Fig. 2c). Slip along the interface acts to blunt the fracture tip.

Teufel and Clark (1984) found that a decrease in friction along the interface requires a higher interface-normal compressive stress in order for the fracture to propagate across the interface. Renshaw and Pollard (1995) followed up on these observations to develop a criterion for fracture termination at weak interfaces based on remote stresses and interface friction. Once slip occurs along the interface, Renshaw and Pollard (1995) assumed that tensile stresses are no longer transmitted across the interface and fracture growth is prohibited. Their resulting criterion for fracture propagation across a frictional interface relates the remote normal stresses to tensile strength of the rock and interface friction. Interface slip and subsequent fracture termination are more likely to occur at low values of coefficient of friction and remote interface-perpendicular compression (Renshaw and Pollard, 1995). Additionally, Renshaw and Pollard (1995) noted that in many cases the crossing fracture does not develop just ahead of the initial fracture but to either side, forming a step-over fracture. The conditions for step-over were not explored in their experimental study.

1.2. New fracture initiation along bedding contacts

We investigate the potential for fracture propagation across, termination at, or step-over at a bed contact by examining the stresses along this contact as the fracture approaches the contact. If the stresses are great enough, a new fracture will initiate along the intact side of the bedding contact, resulting in either fracture step-over or fracture propagation across the contact. Generally, a new fracture initiates if the maximum tensile stress (maximum principal stress) on the intact side of the interface exceeds the tensile strength of the material (e.g. Jaeger and Cook, 1979). This study utilizes the tension positive sign convention to ease analysis of fracture propagation and initiation, which develop under tensile stresses. However, maximum tension is not the only consideration for fracture initiation. Fractures typically initiate at local concentrations of tensile stress around flaws, such as fossils (e.g. Pollard and Aydin, 1988). Since larger flaws produce greater stress concentrations, the location of fracture initiation depends on the distribution of the largest flaws as well as the magnitude of maximum principal tension (Gross, 1993). In beds with evenly distributed flaws, fracture initiation occurs where tensile stresses are the greatest (Gross et al., 1995).

The distribution of maximum tension near a fracture tip highlights the potential for fracture initiation off the plane of the parent fracture (Fig. 3). Flaws to either side of the fracture experience greater tension than flaws directly ahead of the fracture. For a population of similar flaws, new fractures are expected to initiate off the plane of the parent fracture, resulting in fracture jogs or step-overs (Helgeson and Aydin, 1991). However, step-over fractures are rarely observed within homogeneous materials. In these materials, planar cracks are believed to propagate by coalescing with microcracks in the process zone just ahead of the crack (Hoagland et al., 1973; Delaney et al., 1986; Lawn, 1993), rather than with small off-plane fractures that might initiate at locations of maximum tension. Thus, the presence of microcracks in the inelastic process zone ahead of the propagating fracture suppresses step-over of fractures in homogeneous materials.

Although step-over fractures are not observed within homogeneous rocks, they have been observed at sedimentary bed contacts in the field (Fig. 1; Helgeson and Aydin, 1991) and at interfaces within experiments (Renshaw and Pollard, 1995). Deformation along these contacts must alter the stress field along the intact side of the contact in a such a

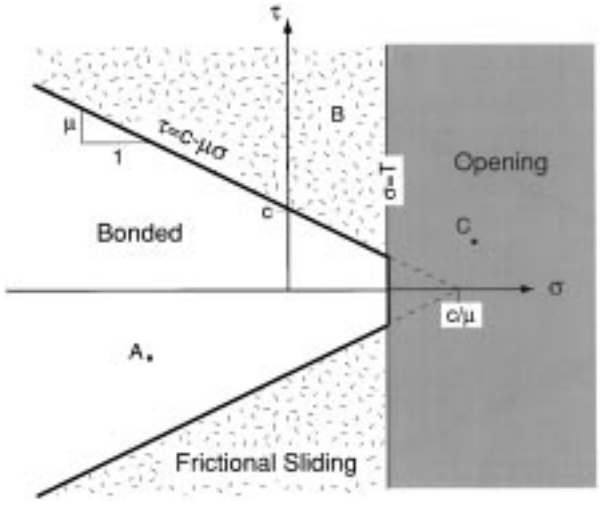

Fig. 4. Conceptualization of the interface constitutive properties in shear–normal (τ–σ) stress space. Where the shear stress does not exceed the Coulomb friction criterion, for example point A, the interface element is bonded. Point B lies within the ornamented region where shear stress exceeds the frictional sliding criterion and the element represented by B slips. Where the normal stress exceeds the tensile strength of the interface, T, within the dark shaded region (e.g. point C), the interface opens.

way that step-over fractures develop rather than planar propagation due to microcracking within the process zone ahead of the crack. Helgeson and Aydin (1991) proposed that greater distance from the parent crack to the position of greatest maximum tension promotes the development of fracture step-overs rather than fracture propagation through the interface. Furthermore, they used numerical models to evaluate the influence of inelastic deformation of a thin shale layer on the potential step-over distance of fractures propagating through siltstone layers bounding the deforming shale. The magnitude of this distance depends on the size and distribution of flaws within the siltstone, as well as the mechanics of stress transfer between siltstone beds (Helgeson and Aydin, 1991).

These field, experimental, and numerical studies suggest that deformation along interfaces may promote both new fracture initiation away from the fracture tip as well as fracture termination at the interface. While the laboratory experiments focused on interlayer slip, interface opening also likely occurred. Consequently, both mechanisms of interface deformation (sliding and opening) are further explored within our study.

We use numerical experiments to investigate two potential mechanisms for fracture termination at, propagation through, and step-over at bedding contacts: (1) debonding and subsequent opening of bed contacts (Fig. 2b); and (2) slip along contacts (Fig. 2c). This study only considers the intersection of layer-perpendicular opening-mode fractures with bedding contacts; however, the same mechanisms that terminate bedding-perpendicular fractures may also act on bedding-oblique fractures, such as those observed on fold limbs (Cooke et al., 2000).

2. Numerical modeling

Numerical modeling techniques used in rock mechanics applications typically use the Boundary Element Method (BEM) or the Finite Element Method (FEM). Each method solves the governing differential equations of continuum mechanics for a Boundary Value Problem (Crouch and Starfield, 1990). The BEM simplifies the problem by only requiring the external and internal boundaries of the domain to be discretized, and is well suited for fracture investigations in homogeneous materials. Within the BEM, the boundary is divided into a number of elements where solutions match the prescribed conditions at the midpoint of each boundary element. Once conditions along the boundaries are solved, the stresses or displacements along the boundary, and the stresses, strains and displacements anywhere within the body can be found.

A special type of BEM, the displacement discontinuity method, is particularly useful for modeling deformation associated with cracks. Using this method, each element has constant slip and opening along its length. The analytical solution for a single, constant displacement discontinuity can be used to build the solution to any discretized problem by summing the influence of all elements (Crouch and Starfield, 1990).

In this project, numerical modeling of a fracture approaching a frictional interface utilizes the BEM code developed by Cooke (1996), called FRIC2D. FRIC2D is a numerical code developed to analyze frictional slip and associated opening-mode fracture propagation in two dimensions. Stress and displacement calculations are based on the boundary element program TWODD developed by Crouch and Starfield (1990), which employs the displacement discontinuity method. FRIC2D incorporates inelastic frictional slip via special constitutive interface elements that simulate frictional slip along weak bedding surfaces (Cooke, 1996).

Unlike regular boundary elements that require specification of stresses or displacements, these constitutive interface elements require prescription of constitutive properties (Crouch and Starfield, 1990). The constitutive properties of these elements include shear stiffness, normal stiffness, cohesion (c) and the coefficient of friction (μ). The elastic interface parameters, normal and shear stiffness, are analogous to the shear and Young moduli for bulk material, because the normal and shear stiffness relate the normal (σ) and shear (τ) stresses to the normal and shear displacements along the interface. At low stresses the interface deforms elastically, whereas at greater shear or tensile stress the interface may slip or open inelastically (i.e. non-reversibly). Within FRIC2D, interface elements slip where the Coulomb friction criterion is met,

$$|\tau| \geq c - \sigma\mu. \tag{1}$$

In the presence of tensile stresses, the interface may open.

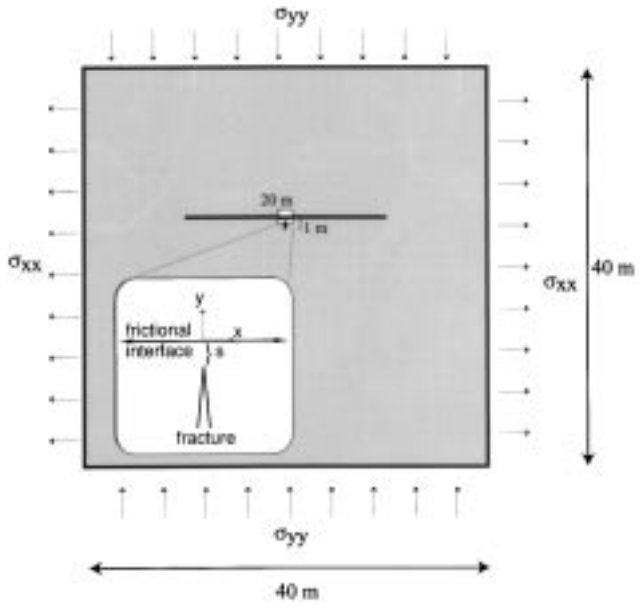

Fig. 5. Model used to examine fracture termination at weak mechanical interfaces. The model includes four outer boundaries along which remote stresses (σ_{xx} and σ_{yy}) are specified, a horizontal interface and a vertical fracture that grows longer as it approaches the interface. The distance from the interface to the far tip of the fracture is 1 m. The inset shows an enlargement of the fracture tip region.

Within FRIC2D, the interface elements open where the normal stress across the interface exceeds the tensile strength of the interface, T,

$$\sigma \geq T. \tag{2}$$

If $T < c/\mu$, this opening criterion is implemented as a tensile cut-off to the frictional slip criterion (Fig. 4) in a similar fashion as the tensile cut-off of the Mohr–Coulomb failure envelope for intact rock (e.g. Goodman, 1989). Once the tensile strength of the interface is exceeded, the bonding and/or cementation of the interface is broken, reducing the subsequent tensile strength of the interface. Within FRIC2D, this debonding of interface elements is simulated by applying zero shear and normal tractions along interface elements that have exceeded the interface tensile strength and consequently have opened.

Once any element slips or opens, the stress state of the entire system must be recalculated because slip or opening of one element will change the state of stress on neighboring elements, which in turn may also slip or open (Cooke and Pollard, 1997). This process is repeated until the differences in shear stresses and normal stress of successive iterations falls below a prescribed tolerance level (Cooke and Pollard, 1997). For this study we used a tolerance of 0.1% in all models. Once the tolerance is met for both slip and opening, the solution is considered to have converged.

Some previous studies using the constitutive elements of FRIC2D investigated frictional slip along bedding planes (Cooke and Pollard, 1997; Cooke et al., 2000), propagation of blind thrust faults (Roering et al., 1997), and fracturing associated with frictional slip along faults (Cooke, 1997). The incorporation of interface opening and the associated coding required to ensure model convergence during opening are innovations of this study.

3. Model set-up

To evaluate the contributions of interface slip and debonding to fracture termination and step-over at bedding contacts, we perform numerical experiments on each of these processes, as well as the combination of sliding and opening. The two-dimensional model contains a vertical opening-mode fracture that increases in length as it approaches a horizontal interface representing a bedding contact (Fig. 5). To investigate the fracture approach to the interface, the distance between the interface and the fracture tip, s, and the fracture length, $2a$, are varied so that $2a + s = 1$ m (Fig. 5). Rigid body translation and rotation of the model were minimized. Uniform remote vertical compression simulates overburden loading while propagation of the vertical fracture is driven by remote horizontal tension.

This study was motivated by the author's observations and statistical analysis of fracture termination at bed contacts in the Silurian dolomite of Door County, Wisconsin (Underwood, 1999). For this reason, material properties and boundary conditions are chosen to simulate fracture conditions within the Silurian dolomite. The fractures within the Silurian dolomite may have formed during uplift and subsequent horizontal extension of the strata in the presence of elevated pore pressures (Underwood, 1999). We estimate the depth of burial during fracture development to be around 200 m (−5 MPa) and the effective horizontal tension to be around 5 MPa. Although pore pressure is not explicitly considered within this model, the effective horizontal tension may incorporate the influence of pore pressure on fostering fracture propagation. Material parameters for the Silurian dolomite (Young's modulus: 65 GPa; Poisson's ratio: 0.35) were assigned based on published results from analogous materials (Birch, 1966). While the numerical experiments simulate a particular situation, the results can be generalized, as will be shown in the Discussion.

3.1. Element size and boundary location

The suitable element size and boundary location for the model can be assessed by inspecting the analytical solutions for a crack in tension. The analytical solution for deformation around a 1-m-long, open crack within a homogeneous, isotropic and linear-elastic body subjected to 5 MPa uniform remote tension normal to the crack can be derived from the Westergaard function (e.g. Tada et al., 1985). This solution can also be used to check the numerical model and assess the error of the numerical experiments (see Section 3.2).

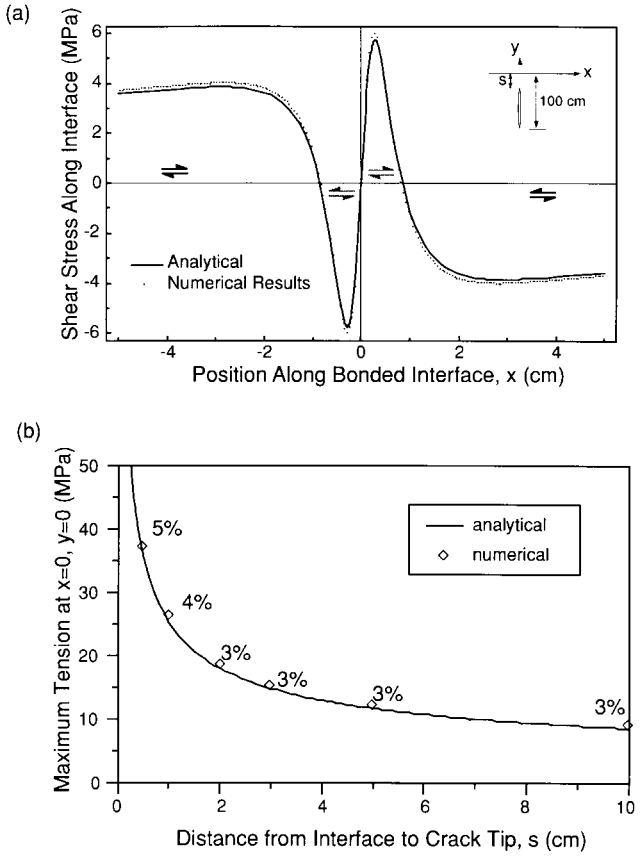

Fig. 6. (a) Shear stress along the interface when the fracture tip is $s = 0.5$ cm from the interface. (b) Comparison of analytical solution with numerical results highlights the errors incurred by discretization.

The Westergaard solution shows that deformation 10 m away from the 1-m-long crack is not significantly influenced by the presence of the crack. Thus, such a distance is appropriate for the outer boundaries of our model, but to be conservative, we placed the boundaries of the model 20 m to either side of the fracture (see Fig. 5). For similar reasons, the interface representing the bedding contact extends 10 m to either side of the opening fracture. Sensitivity tests of varied element length showed that elements smaller than 0.5 m along the model boundaries did not significantly influence opening along the crack. So, this element length is used along the boundaries.

The element length along the fracture and the interface must be small enough to capture the intricacies of deformation near the fracture tip, where slip and debonding will be localized. Furthermore, this length is most critical when the fracture tip is closest to the interface. The shear stress distribution is more complex than the normal stress distribution because of reversals in shear direction (Fig. 6a). Therefore, to simulate interface deformation accurately when the fracture tip is 0.5 cm from the interface (the closest condition considered in this analysis), the interface element size is limited to 0.5 mm within 25 cm to either side of the fracture. Outside of this zone, the interface element length is 2.5 cm. Fracture elements are similarly scaled: the upper half of the fracture has 0.5-mm-long elements while the lower half has 2.5-cm-long elements. Using small equal-length elements everywhere along the boundaries, fractures, and interfaces minimizes errors in the stress/displacement calculations (Crouch and Starfield, 1990). However, the available CPU limits the number of elements we can reasonably use. For this reason, larger elements are used far from the area of interest, such as along the boundaries away from the fracture–interface intersection. This size distribution for the elements reduces the total number of model elements and reduces the stress/displacement calculation errors near the fracture.

3.2. Error assessment

Model testing via comparison of model results with analytical solutions ensures that numerical errors due to the presence of model boundaries and discretization do not contribute significantly to the model results. We performed the test by examining the maximum tension along a bonded interface just ahead of the fracture ($x = 0$). The numerical model used for this comparison with the analytical solution incorporated a bonded interface along which opening and sliding are inhibited to approximate the homogeneous host rock of the analytical solution. Furthermore, this particular model examined a crack subjected to an isotropic 5 MPa remote tensile stress due to the constraints of the analytical solution. All other models in this study examine an anisotropic remote stress field with −5 MPa vertical normal stress and 5 MPa horizontal tension. The maximum tension along the interface just ahead of the crack ($x = 0$) increases rapidly as the crack approaches the interface (Fig. 6b). For a crack subjected to an isotropic 5-MPa remote tensile field and a fracture tip 0.5 cm or farther from the interface, the numerical approximations for maximum tension along the interface ahead of the crack are within 5% of the analytical solution (Fig. 6b). These relatively small discrepancies may result from numerous sources, including discrete and non-uniform element lengths used within the numerical models. We consider errors of 5% or less suitable for this study.

3.3. End-member model conditions and interface strengths

This study assesses end-member conditions for fracture intersection with bedding contacts by investigating first the case of interface slip with no opening (sliding-only) and then the case of debonding and subsequent opening along the interface with no sliding (opening-only). The combination of opening and slip is investigated in the third suite of models.

Within each suite of models, several different interface conditions are examined to explore the nature of fracture propagation, termination or step-over with respect to different strength interfaces. Strong interfaces are simulated

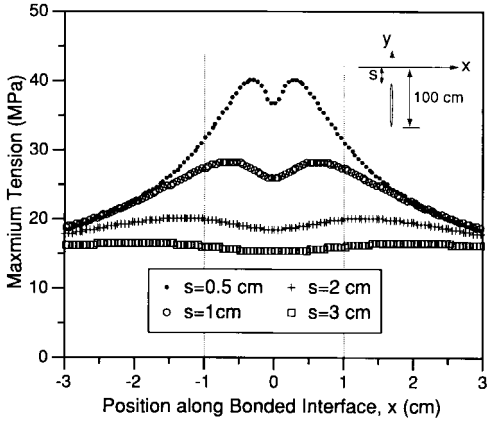

Fig. 7. Maximum tensile stress along a bonded interface. Maximum tension increases as the fracture approaches the interface. The greatest tension occurs to either side of the parent fracture and moves closer to $x = 0$ as the fracture approaches the interface.

with very high values of friction coefficient, cohesion and tensile strength. Since these strong interfaces neither open nor slide within the model, the interfaces are considered to be bonded or welded. In contrast, very weak interfaces will slide easily under non-zero shear stress and open easily under interface tension. Such behavior is simulated by $\mu = 0$ and $c = 0$ MPa in the sliding-only interface models, $T = 0$ MPa in the opening-only interface models, and finally $\mu = 0$, $c = 0$ MPa and $T = 0$ MPa within the combination sliding and opening models. Between the end-members of bonded and weak interfaces lies what we have termed moderate-strength interfaces. For the purpose of this study, moderate-strength interfaces are simulated with a friction coefficient based on rock contact friction experiments, $\mu = 0.65$ (Byerlee, 1978), and strength values of $c = 3.25$ MPa and $T = 5$ MPa. Because strength data for bedding interfaces are not available, we use values that are fractions of the average strength of intact rock (~10 MPa, Goodman, 1989; Suppe, 1985). Moderate-strength interfaces slip only where the frictional slip criterion (Eq. (1)) is met in the sliding-only and combination models, and open only where the tensile stress across the interface exceeds T (Eq. (2)) in the opening-only and combination models.

The three suites of models seek to isolate the influence of interface slip and interface opening on fracture propagation through, termination at, and step-over at bedding interfaces. Because the models strive to isolate one or other mechanism of interface deformation rather than simulating natural conditions, all three suites of models incorporate interface shear and normal stiffnesses several orders of magnitude greater than the rock stiffness. The high interface normal and shear stiffnesses minimize elastic deformation along the interface so that the resulting behavior is limited to slip and opening due to stresses that meet the prescribed interface sliding and opening criteria.

4. Model results

To investigate the potential for fracture propagation through, termination at or step-over at sliding and opening interfaces, we examine the maximum principal tensile stress along the top of the interface (the intact side of the interface). Along a bonded interface, two locations of greatest principal tension exist to either side of the fracture (Figs. 3 and 7). These peaks are most pronounced when the fracture is within 1 cm of the interface and the greatest principal tension occurs along the interface within 1 cm of $x = 0$ (Fig. 7). However, if the interface slips and/or opens the magnitude and position of greatest principal tension will differ. To determine whether the fracture will propagate through slipping/opening interfaces, we compare the patterns of greatest maximum tensions in those cases to that produced along bonded interfaces. Because fractures are observed to propagate straight through bonded interfaces (through $x = 0$), we assume that if the greatest value of maximum tension along the sliding/opening interface develops within ~1 cm of $x = 0$, and the magnitude of the greatest maximum tension meets or exceeds that along the bonded interface, the fracture will propagate through the interface at $x = 0$. If the greatest value of maximum principal tension is less than that along the bonded interface, the fracture may terminate at the interface. If the greatest maximum principal tension along sliding/opening interfaces occurs at $|x| > 1$ cm, a new fracture may develop along the top of the interface that steps-over from the parent fracture.

Once the interface slips, the maximum tensile stress along the bottom of the interface differs from that along the top of the interface due to the anti-symmetry of stresses around a sliding fracture (e.g. Lawn, 1993). The greatest maximum tension along the bottom of the interface could exceed the greatest maximum tension above the interface to either side of the parent fracture. Under such conditions, flaws along the bottom of the interface would initiate fractures that propagate downwards from the interface. Because these new fractures would propagate into the stress shadow of the parent fracture, their propagation may be arrested due to lack of driving stress, so that they do not extend far into the layer (Nemat-Nasser et al., 1978; Pollard and Aydin, 1988; Gross et al., 1995). Alternatively, the fractures growing from the bottom of the interface might propagate to link up with the parent fracture. Although these scenarios warrant further investigation, we are interested in the development of new fractures above the interface and correspondingly limit our analysis to fracture development there.

4.1. Sliding-only interface models

The fracture approaching the interface imposes shear stresses along the interface that promote slip. To evaluate the influence of interface slip on fracture propagation through, termination at, and step-over at bedding interfaces,

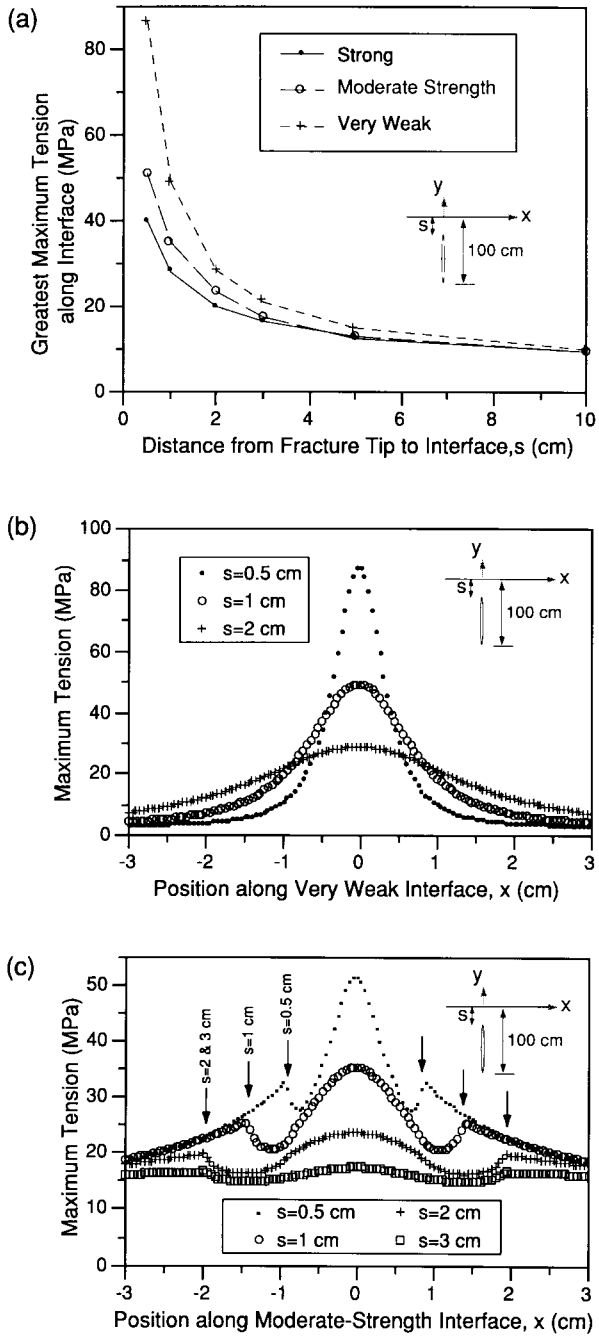

Fig. 8. (a) Greatest values of maximum tensile stress along the bonded and sliding-only interface models. Distribution of maximum tension along the very weak (b; $\mu = 0$; $c = 0$ MPa) and moderate-strength (c; $\mu = 0.65$; $c = 3.25$ MPa) interfaces. The ends of slipped segments of the moderate-strength interface are marked with arrows.

we investigate several models where interface deformation is limited to sliding (i.e. there is no opening along the interface). Within the numerical experiments, constitutive interface elements are used to examine two conditions, an interface infinitely weak in shear (freely sliding interface: $\mu = 0$; $c = 0$ MPa) and a moderate-strength, frictionally sliding interface ($\mu = 0.65$; $c = 3.25$ MPa). A modification was required for the moderate-strength interface ($\mu = 0.65$; $c = 3.25$ MPa), which deforms by inelastic frictional slip, because those models would not converge to a solution. Convergence was impeded along about 12 interface elements within $-0.275\text{ cm} < x < 0.275\text{ cm}$ that were numerically unstable and flipped from one slip sense to another between convergence iterations. To avoid this problem and allow stable convergence, frictional elements were allowed to slide freely where tensile stress across the interface exceeds 5 MPa. Under this relaxed frictional slip condition, several elements near $x = 0$ slide freely when the fracture is 3 cm from the moderate-strength interface. When the fracture is within 0.5 cm of the interface, free slip occurs only along elements within $-0.6\text{ cm} < x < 0.6\text{ cm}$ along the moderate-strength interface.

Deformation along both weak and moderate-strength interfaces is investigated as the tip of a vertical fracture approaches the interfaces ($10\text{ cm} > s > 0.5$ cm). The weak interface begins to slip freely when the fracture is 5 cm from the interface, whereas the moderate-strength interface does not slide until the fracture is 3 cm from the interface. The greatest values of maximum tensile stress along the top of both the weak interface ($\mu = 0$; $c = 0$ MPa) and moderate-strength interface ($\mu = 0.65$; $c = 3.25$ MPa) occur near $x = 0$ and far exceed the greatest maximum tensile stress along a bonded interface (Fig. 8a).

Interface left-lateral slip along $x < 0$ and right-lateral slip along $x > 0$ along the moderate-strength interface have small magnitudes (Fig. 9), but contribute to significant changes in the stresses along the top of the sliding interface (Figs. 8c and 9). The increase in maximum tensile stress along the top of the sliding interface near $x = 0$ is partly a consequence of the shear-sense reversal at this location imposed by the fracture tip stress field (Fig. 9). The increased tensile stress above the interface promotes the co-planar initiation of a new fracture on the intact side of the interface (Fig. 9).

In addition to a peak in the maximum tension at $x = 0$, the moderate-strength interface ($\mu = 0.65$; $c = 3.25$ MPa) has smaller peaks that occur near the tips of the sliding segments (arrows in Fig. 8c). These peaks are associated with changes in slip magnitude at the ends of the sliding segment. Local stress concentrations along sliding fractures are associated with regions of high slip gradient (e.g. Cooke, 1997); however, in this case, the stress concentrations act to lower the maximum tensile stress. Left-lateral slip along $x < 0$ and right-lateral slip along $x > 0$ impose compressive stresses along the top of the interface at the ends of the slipped segment (Fig. 9), which locally reduce the maximum tension (Fig. 8c). The localized drop in maximum tension near the ends of the slipped interface segment results in a small relative peak at the tip of the slipped segment. This behavior is in contrast to that for an infinitely weak interface, which slides under any amount of shear stress. Thus, the entire length of the modeled weak interface experiences some degree of slip. Consequently, stress is not localized and local peaks in the maximum tension are

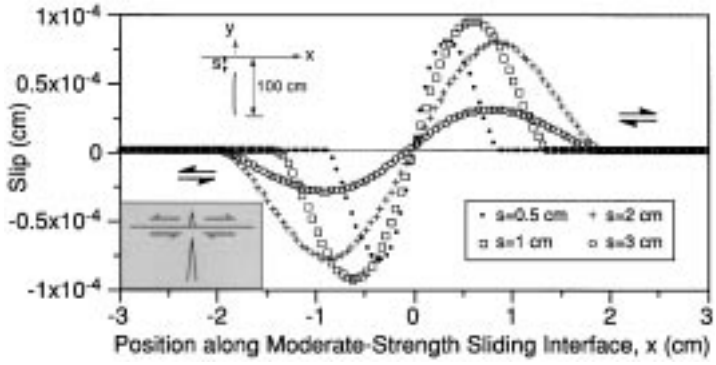

Fig. 9. Slip distribution along the moderate-strength ($\mu = 0.65$; $c = 3.25$ MPa) sliding-only interface. Right-handed slip is positive and left-handed is negative. The inset on the lower left shows the slip-sense reversal at $x = 0$, producing high tensile stresses above the interface at $x = 0$ that promote fracture propagation straight through the interface.

not produced, because of the lack of abrupt change in slip amount.

The moderate-strength interface has the greatest value of maximum tension at $x = 0$, but the pronounced peak in this location may be partly a consequence of free-slip along several elements near $x = 0$. Possibly, the moderate-strength interface with fully converged frictional slip would have two peaks in maximum tension, similar to the bonded interface. Yet, further exploration of this issue necessitates the development of more advanced modeling tools that are beyond the scope of the present work.

Because we restrict opening along both the weak and moderate-strength sliding interfaces, normal stresses are transmitted across the interfaces. The transmission of these normal stresses may contribute to elevating the maximum tensile stress along the top of the interface at $x = 0$. If both slip and opening were permitted along the interface, tensile stresses above the interface would decrease, perhaps precluding fracture development. The effect of a combination of sliding and opening is explored in the third suite of numerical experiments.

In summary, along both infinitely weak and moderate-strength sliding interfaces, the maximum tensile stress exceeds that for the bonded interface and occurs in front of the fracture at $x = 0$ along the interface (Fig. 8). These results suggest that interface sliding alone enhances the likelihood that fractures propagate through bedding contacts. This result, however, is not consistent with our observations that fractures often terminate at non-bonded bedding contacts. Therefore, another mechanism must be responsible for the termination of fractures in rock strata, and our original supposition that slip alone along bedding could act to blunt the crack tip (e.g. Fig. 2b) is not substantiated.

4.2. Opening-only interface models

As a fracture propagates toward an interface, tensile stresses develop across the interface. Debonding and subsequent opening of the interface occurs when interface-normal tensile stresses exceed the prescribed interface tensile strength. To isolate the influence of interface opening on fracture propagation or termination, we disallow sliding along the modeled interfaces. We analyze two interfaces with different tensile strengths: a very weak interface with zero strength ($T = 0$ MPa) and a moderate-strength interface with 5 MPa tensile strength.

As the fracture approaches the interface, portions of the interface debond and open. The very weak interface ($T = 0$) opens when the fracture is within 5 cm of the interface, whereas the moderate-strength interface ($T = 5$ MPa) does not open until the fracture is within 3 cm. For both interfaces, the length of the open segment decreases as the fracture approaches (where aperture goes to zero in Fig. 10c is shown with arrows in Fig. 10a, b) and stresses become more localized around $x = 0$. The length of the open interface segment depends on interface strength, vertical compression across the interface, and fracture length. For these models with 5-MPa vertical compression, 5-MPa horizontal tension and a ~1-m-long fracture, the open segment along the very weak interface becomes as long as 7.0 cm (3.5 cm to either side) when the fracture tip is 3 cm from the interface. The greatest interface aperture occurs at $x = 0$ and is of the order of 1×10^{-3} cm (Fig. 10c), smaller than one could detect visually in the field.

For both opening-only models, the greatest values of maximum tension develop not in front of the fracture ($x = 0$), but to either side (Fig. 10). The maximum tension occurs near the ends of the open segments when the fracture is far from the interface and occurs within the open segment when the fracture is near. For the very weak interface, this transition occurs as the fracture tip advances from 2 cm to 1 cm away, whereas for the moderate-strength interface, the transition occurs when the fracture is closer to the interface, for $1\text{ cm} > s > 0.5$ cm. The narrow peaks in maximum tension at the ends of the open segments can be explained by considering the deformation around mode I cracks. The tips of these cracks or open segments have stress concentrations that locally elevate the maximum tensile stress along the interface (Fig. 10a, b). Analogous to the slip-sense changes along the sliding-only interface, abrupt

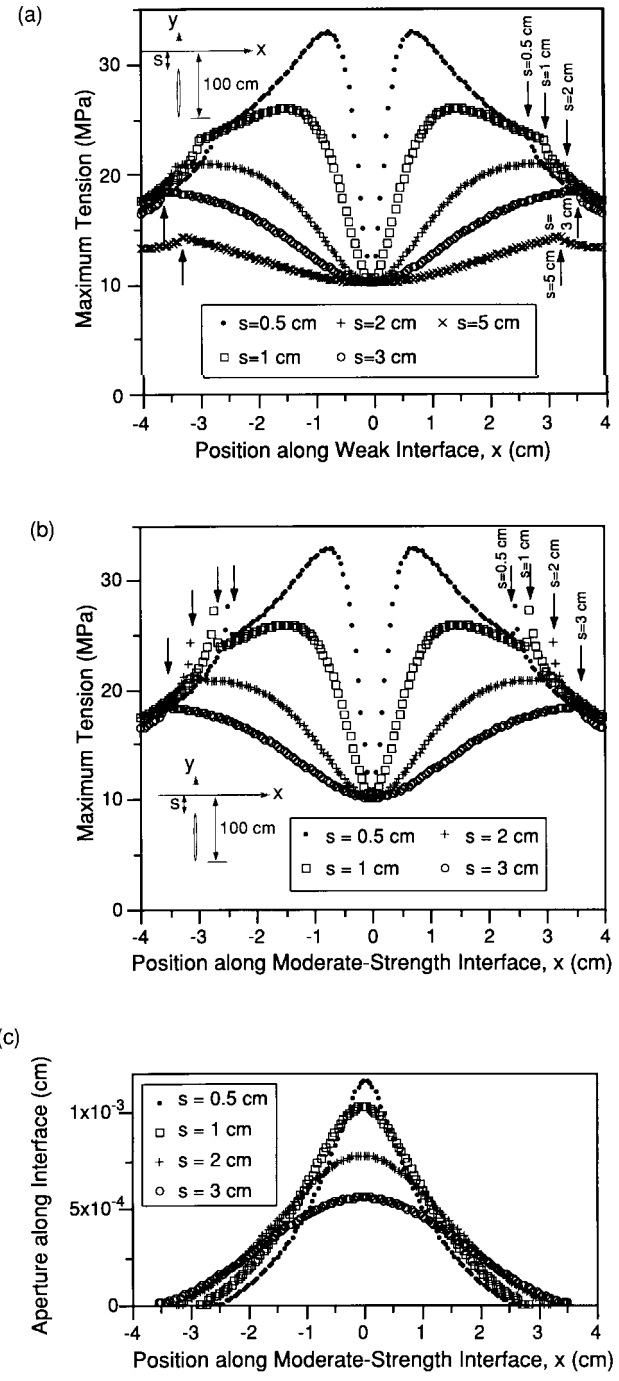

Fig. 10. (a, b) Distribution of maximum tension along very weak (a; $T = 0$ MPa) and moderate-strength (b; $T = 5$ MPa) opening-only interfaces. The locations of the ends of the open interface segments are indicated with arrows. (c) The distribution of aperture along the moderate-strength opening-only interface.

changes in crack aperture produce stress concentrations. Since the weak interfaces open under any amount of tension, these interfaces do not change aperture abruptly and lack local stress concentrations. Thus, the moderate-strength interface has more pronounced peaks in maximum tension than the weak interface (Fig. 10a, b). Similarly, the drop in maximum tension along the moderate-strength interface at $x = 0$ corresponds to the nearly constant interface aperture in this location (Fig. 10c).

The greatest value of maximum principal tension along the top of the interface increases for both the very weak and moderate-strength interfaces as the fracture approaches (Fig. 10). By inspecting the maximum tension along the top of the opening interfaces as the fractures approach, we can assess the types of fracture–bed contact intersection that may result from interface opening. As a fracture grows towards an opening-only interface, the greatest maximum tension first develops at the tips of the open segments. For these models, the range of this location was ~ 2.5 cm $< |x| < \sim 3.5$ cm depending on interface strength and distance to fracture tip. If the maximum tension in this region exceeds the tensile strength of the rock or if there are large flaws at which the stress intensity factor exceeds the fracture toughness of the rock (e.g. Pollard and Aydin, 1988), new fractures will develop to the right and left of the parent fracture. These results suggest that interface opening may be a mechanism responsible for the development of step-over fracture patterns at bedding contacts.

Alternatively, the maximum tension at the ends of the open segments may not be great enough to initiate new fractures. If the fracture grows within 0.5 cm of the interface without initiating a step-over fracture, the greatest value of maximum tension occurs within 1 cm of $x = 0$, rather than at the tip of the open interface segment. Under these conditions, a new fracture may develop that is co-planar with the parent fracture, just as with the bonded interface scenario. Because the greatest maximum tension along the interface 0.5 cm from the fracture tip does not exceed that along the bonded interface (Figs. 7 and 10), fracture propagation through the interface is not guaranteed (as it was for the sliding interface). If the stresses are not great enough to develop a new co-planar fracture, the parent fracture will terminate at the interface.

In summary, opening along bedding contacts provides a compelling mechanism for the development of step-over fractures at bedding contacts. If the stresses are not great enough to initiate new step-over fractures, the parent fracture may terminate at the bedding contact. Within a small range of conditions, when stresses are not great enough to create new step-over fractures but are great enough for through propagation when the fracture is close to a bedding contact, fractures might propagate through the contact.

4.3. Sliding and opening interface models

Along many bedding contacts within rock strata, we expect a combination of opening and frictional slip. This behavior necessitates an additional suite of models that allows both opening and slip. We investigate two interfaces: a weak interface with zero tensile strength and zero shear strength ($\mu = 0$; $c = 0$ MPa; $T = 0$ MPa) and an interface

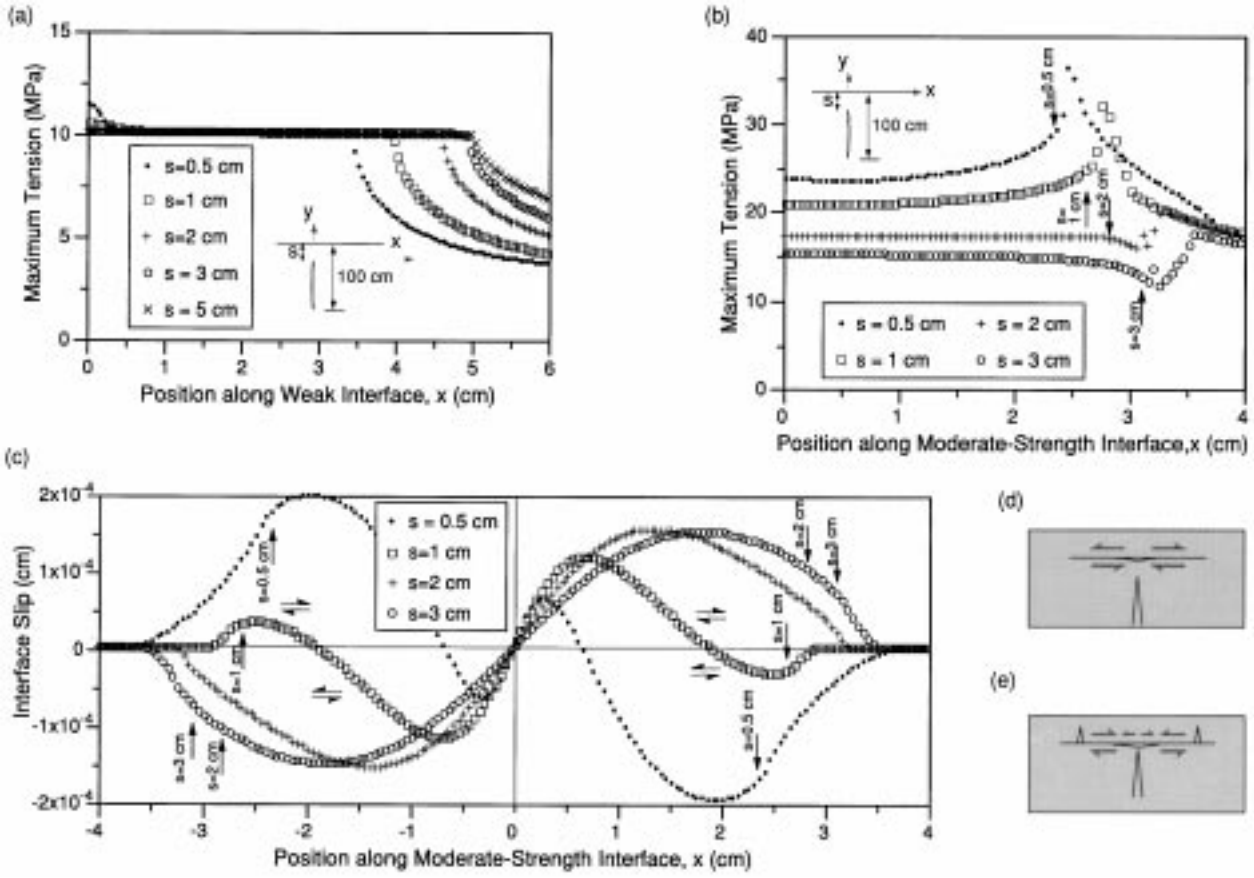

Fig. 11. (a, b) Distribution of maximum tension along very weak (a; $\mu = 0$; $c = 0$ MPa; $T = 0$ MPa) and moderate-strength (b; $\mu = 0.65$; $c = 3.25$ MPa; $T = 5$ MPa) interfaces that deform under combination of sliding and opening. To improve clarity of data presentation, only deformation along the right half of the moderate-strength interface is presented. Arrows indicate position of the tips of open segments along the interfaces. (c) The slip sense and magnitude along the moderate-strength interface change as the fracture approaches the interface. (d) Cartoon showing slip sense along an interface when the fracture is farther from the interface (2 cm $\leq s \leq$ 3 cm). (e) Cartoon showing slip sense along the interface when the fracture tip is close ($s \leq 2$ cm) to the interface.

with moderate tensile strength ($T = 5$ MPa) and moderate frictional strength ($\mu = 0.65$, $c = 3.25$ MPa). When portions of the interface debond ($\sigma > T$), the normal and shear tractions on the debonded elements become zero, so that open segments of the interface in these models experience slip as well as open. Additionally, the tensile strength along debonded elements reduces to zero, which facilitates further opening.

The moderate-strength interface ($T = 5$ MPa; $\mu = 0.65$; $c = 3.25$ MPa) begins to slip and open when the fracture is within 3 cm of the interface, whereas the weak interface ($\mu = 0$; $c = 0$ MPa; $T = 0$ MPa) opens and slips when the fracture is within 5 cm of the interface. A central interface segment opens and slides, and is shouldered by two sliding-only interface segments. Maximum tension is greatly reduced along the central segment of both the weak and moderate-strength interfaces ($x = 0$, $y = 0$; Fig. 11a, b vs Fig. 7). Along the very weak interface, the maximum tensile stress occurs at $x = 0$ ahead of the fracture (Fig. 11) and equals about twice the remote tension. This stress does not equal the remote tension because some stresses are transmitted across the interface to either side of the central segment, even though no stresses are transmitted across it.

Along the moderate-strength interface, the greatest value of maximum principal tension occurs farther than 2.5 cm away from the parent fracture. The length of the central segment decreases as the fracture approaches the interface (arrows in Fig. 11b, c). The outer tips of the slip-only segments that shoulder the central segment move towards the parent fracture as it grows within 1 cm of the interface (where slip approaches zero in Fig. 11c). They move away from the parent fracture as it grows within 0.5 cm of the interfaces (Fig. 11c). When the fracture is 2–3 cm away, the greatest tension along the top of the interface develops in front of the slip-only segments of the interface that shoulders the central segment (Fig. 11b for stress magnitudes, Fig. 11c for tip locations). When the fracture grows within 1 cm of the interface, the greatest tension develops at the ends of the central segment (arrows in Fig. 11b, c), but behind the tips of the slip-only segments.

This behavior can be attributed to the change in slip sense along the slip patches that shoulder the central segment as

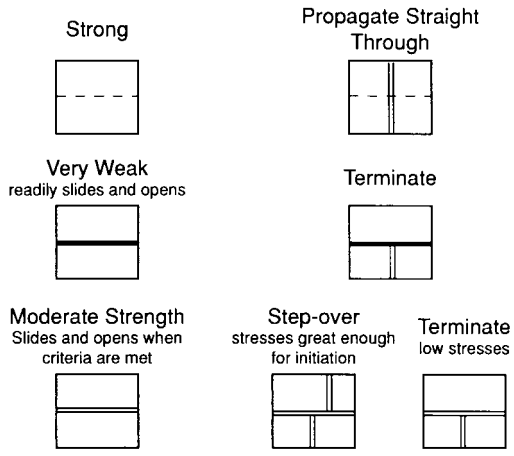

Fig. 12. Inferred variations in geometry of fracture–bed contact intersection for bedding contacts with different strengths.

the fracture propagates toward the interface (Fig. 11c–e). When the fracture tip is far from the interface (e.g. 2 cm $\leq s \leq$ 3 cm), the ends of the central segment lie within the region of right-lateral shear along $x > 0$ and left-lateral shear along $x < 0$ (Fig. 11c, d). This slip sense along the central and shouldering segments reduces tension on top of the interface near the tips of the sliding segments (Fig. 11d). The reduction of maximum tension at the tips of the slip-only segments yields a relative increase in maximum tension ahead of this segment, which produces the small peaks in Fig. 11b; when the fracture lies close to the interface ($s \leq 1$ cm), the shouldering slip-only segments and much of the central segment lie within the outer left-lateral shear sense along $x > 0$ and right-lateral sense along $x < 0$. This slip sense enhances the concentration of tensile stresses above the interface at the tips of the sliding segments (Fig. 11e), producing the pronounced peaks in the maximum tension for the case of $s \leq 1$ cm (Fig. 11b).

Whereas the maximum tension along very weak interfaces is greatly reduced by opening and sliding, moderate-strength interfaces can produce localized regions of large maximum tension to either side of the parent fracture. In summary, the combination of slip and opening along an interface may either terminate fractures at bedding contacts if the contacts are very weak or produce step-over fractures to the left and/or right of the parent fracture if the contacts are moderately strong. If the stresses are not great enough to initiate new step-over fractures across the moderate-strength interface, the parent fracture may terminate at the bedding contact.

5. Discussion

The numerical models within this study assume that the host rock around the fractures deforms as a linear and elastic material. However, this assumption is not valid near fracture tips, where high stresses produce local inelastic yielding of the host material (Lawn, 1993). The zone of inelastic yielding (process zone) scales with fracture size so that a 1-m-long fracture has a process zone of ~1 cm (e.g. Broek, 1991). As the fracture tip approaches within 1 cm of the interface, local failure via microcracking and other mechanisms reduce stresses along the interface. Thus, the stresses reported here for distances less than 1 cm from the interface are likely to be greater than those experienced along natural bedding contacts. Interestingly, for the case of a 1-m-long fracture at 200 m depth, the maximum tensile stress along the interface is great enough to produce new step-over fractures when the fracture tip is still 5 or 10 cm from the interface (and neither opening or slip has yet occurred). Although in thinner beds the fracture would need to be closer to the interface before new fractures develop, the fracture may not necessarily need to be as close as the length of the process zone.

5.1. Expected types of fracture intersection with bed contacts

The numerical models of this study explore the influence of several end-member mechanisms and interface strengths on fracture intersection with sliding and opening interfaces. The model results can be used to infer fracture termination at, propagation through, and step-over at different types of bedding contacts (Fig. 12). Bedding contacts that are strongly welded or well cemented, such as gradual contacts and reworked (e.g. bioturbated) contacts, may be approximated by bonded interfaces. The model results suggest that most fractures would propagate through such contacts (Fig. 12). Fracture propagation has been observed through bedding contacts that silicified during diagenesis and appear well cemented (Underwood, 1999). In contrast to strongly cemented contacts, some bedding planes, such as laminated organic partings, have very little cementation and may be approximated by interfaces that are very weak in both shear and opening. The model results suggest that such contacts would terminate propagating fractures (Fig. 12). Fracture termination has been observed at weak contacts such as unmineralized pre-existing joints (Dyer, 1988; Gross, 1993), thin organic layers (Underwood, 1999), and uncemented bedding contacts (Narr and Suppe, 1991; Becker and Gross, 1996).

Most sedimentary bed contacts are neither strongly bonded nor infinitely weak. The numerical experiments simulate such contacts with moderate-strength interfaces ($\mu = 0.65$; $c = 3.25$ MPa; $T = 5$ MPa) that are permitted to both open and slide when the debonding and sliding criteria are met. The model results suggest that fractures approaching moderate-strength contacts may either produce step-over fractures across the contact or terminate at the contact if the stresses are insufficient to initiate new fractures (Fig. 12). Step-over fractures have been observed in laboratory experiments (Renshaw and Pollard, 1995) and recognized in the field (Helgeson and Aydin, 1991) as part of

composite joints. The development of right- or left-stepping fractures depends on the distribution of flaws within the regions of elevated maximum tension.

Some important factors that control fracture intersections with bedding contacts, such as depth of burial, driving stress and fracture length, have not been directly assessed within these models. Increased interface normal compression encourages fracture propagation through the interface (Teufel and Clark, 1984; Renshaw and Pollard, 1995). Although Renshaw and Pollard (1995) hypothesized that reducing the interface normal compression promotes fracture termination due to increased interface sliding, the model results of this study suggest that localized interface opening rather than sliding is responsible for fracture termination. Because contact slip and opening are both inhibited at greater burial depths, the influence of greater depth is comparable to increasing the strength of the contacts. Deep burial could suppress the small and localized contact opening that acts to terminate fractures and promote either step-over fractures or fracture propagation through weak and moderate-strength interfaces.

The length of fractures also controls the nature of fracture–bed contact intersection. Increases in fracture length are associated with increases in stress concentration (e.g. Lawn, 1993). The longer fractures in thicker beds would produce greater stress concentrations and greater levels of local slip and opening along contacts with adjacent beds than bed-normal fractures in thinner beds. An increase in the length of opening and sliding segments along the contacts increases the distance from the parent crack to the peaks in maximum tension that may produce new step-over fractures. Thus, thicker layers may be associated with greater amounts of fracture step-over.

Increased stress concentrations are also associated with fractures under greater driving stress (e.g. Lawn, 1993). Greater layer-parallel effective tension increases both the stress concentration associated with the parent crack as well as the overall tension within the adjacent intact beds. This combined influence produces localized regions of tension within the adjacent beds and encourages propagation of fractures from existing flaws in these regions. Increased driving stress either in the form of increased remote tension or elevated fluid pressures would promote the development of step-over fractures and through fracture propagation. Additionally, increased levels of opening and sliding along the interface due to increased driving stress would increase the step-over distance of fractures.

This study did not examine deformation once the fracture intersects the interface. Since the stresses along the interface far exceeded the tensile strength of average rock prior to fracture intersection with the interface, the new fracture would initiate prior to this intersection. However, a qualitative consideration of this intersection in the case of fluid-driven growth may be illustrative. If the fracture growth is driven by fluid pressures, we might expect this fluid to enter the bed contact upon fracture propagation to the interface. Once the fluids have entered the contact, the volume available to the fluid greatly increases. Unless there is additional influx of fluids, the fluid pressure would drop, preventing further propagation. Thus, in the case of relatively rapid propagation of a fluid-filled fracture, some new fractures may develop within the intact rock prior to the fracture intersecting the bedding contact. Yet, after intersection and dispersion of fluid pressure, these small fractures might arrest. Fluid pressures may therefore encourage fracture termination by facilitating interface opening. Thus, fractures driven by fluid pressure may be more likely to terminate against bedding contacts than fractures driven by equivalent remote layer-parallel tension.

In summary, fracture termination is more likely under conditions of shallower depth, lower effective layer-parallel tension (i.e. greater effective layer-parallel compression), and fluid-driven fracture propagation. Furthermore, thicker beds and greater layer-parallel tension may produce greater amounts of step-over than thinner beds and more compressive layers.

5.2. Implications for outcrop-scale fracture patterns

The overall pattern of fracturing with a series of sedimentary beds depends on the mechanical stratigraphy of the strata (e.g. Corbett et al., 1987; Gross et al., 1995; Becker and Gross, 1996; Hanks et al., 1997). This mechanical stratigraphy is controlled not only by the strength of the interfaces, but also by the thicknesses and material properties of the beds (Corbett et al., 1987; Gross et al., 1995). Field investigations demonstrate that, for many different rock types, the fracture spacing roughly equals bed thickness (Price, 1966; Hobbs, 1967; McQuillan, 1973; Huang and Angelier, 1989; Narr and Suppe, 1991; Gross, 1993; Gross et al., 1995; Wu and Pollard, 1995; Becker and Gross, 1996). A variety of theories have been offered to explain the empirical trend as well as observed variations of this trend (Hobbs, 1967; Gross et al., 1995; Wu and Pollard, 1995; Ji and Saruwatari, 1998; Ji et al., 1998; Bai and Pollard, 2000). This empirical relation between fracture spacing and bed thickness can be used with inferences derived from the model results (Fig. 12) to assemble a hypothetical outcrop-scale fracture network for strata incorporating different strength interfaces (Fig. 13). To construct the hypothetical fracture network, we assume fractures propagate through strong contacts, step-over at moderate contacts, and terminate at weak contacts. Right- or left-stepping step-over fractures were chosen randomly along the moderate-strength interfaces. The spacing of fractures in each layer of Fig. 13 correlates to the mechanical unit thickness. For example, the lower strong contact does not act as a mechanical interface so that the thickness of the lowest mechanical unit (and corresponding fracture spacing) incorporates the thickness of both of the two lowest sedimentary layers in Fig. 13.

Not every fracture intersecting the moderate-strength

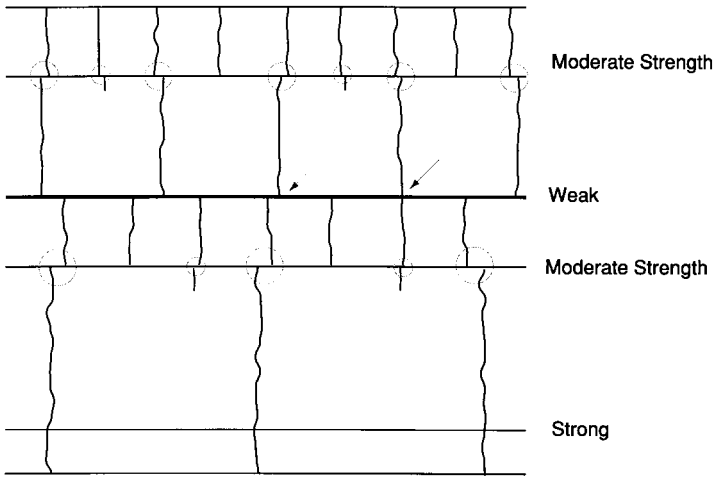

Fig. 13. Hypothetical pattern of fractures within a series of beds separated by different strength interfaces. Circles highlight occurrences of step-over fractures due to opening along the moderate-strength interfaces and circle size correlates with distance of fracture step-over. The spacing of fractures is approximated from the mechanical bed thickness. Apparent step-overs along the weak interface (indicated with arrows) result from the coincidental alignment of fractures among beds. The distinction between coincidental alignment and step-over is difficult to assess without characterization of fracture surface textures (i.e. signatures of propagation direction), relative interface strength (to guide probable intersection mechanisms), and consistencies in fracture pattern along bedding contacts.

contacts steps over these contacts. The fractures propagating within thinner layers are unlikely to initiate step-over fractures in adjacent thicker layers once the fracture spacing within the thicker layers equals the mechanical unit thickness, i.e. once fracture spacing becomes saturated (Narr and Suppe, 1991; Wu and Pollard, 1995). The local stress shadow that develops around fractures inhibits the development of addition fracture near the first (e.g. Pollard and Segall, 1987; Gross et al., 1995). Small step-over fractures are possible but they would not cross the entire length of the thicker beds. Conditions of fracture oversaturation, where fracture spacing is smaller than the layer thickness, may be possible by mechanisms of sequential infilling of unfractured regions with new fractures under additional extensional strain (e.g. Becker and Gross, 1996). Becker and Gross (1996) show that continued sequential in-filling beyond fracture saturation may lead to the localization of high strain and the development of multilayer joints that span multiple mechanical units. The mechanism of step-over fracture at bed contacts may promote the development of multilayer joints by providing initial sub-alignment of some fractures, which may serve to precipitate strain localization.

The outcrop-scale consideration of fracture network development demonstrates that not all fractures step-over at moderate-strength contacts. This behavior impedes the recognition of the step-over mechanism in the field. Fig. 13 demonstrates hypothetical scenarios of coincidental alignment or sub-alignment of fractures (indicated with arrows) and non-coincidental step-over of fractures (indicated with circles). Geologists observing fractures separated by several centimeters within a network, such as those shown in Fig. 13, might interpret them as separately developed fractures that sub-aligned by coincidence rather than the result of one propagation event. One may be able to distinguish between coincidental fracture alignment and fracture step-over sub-alignment by carefully noting fracture surface textures, characterizing the relative strength of the contacts and/or noting consistencies in fracture intersection along particular bed contacts. Fracture surface textures, if available, can be used to determine the direction of fracture propagation (Kulander et al., 1979; DeGraff and Aydin, 1987; Pollard and Aydin, 1988; Helgeson and Aydin, 1991). For example, the interpretation of step-over propagation of sub-aligned fractures is not consistent with the observation that parent and daughter fractures display fracture surface textures that indicate contrasting propagation direction (e.g. up-section vs down-section). Indicators of propagation direction can only be used to rule out step-over propagation but not coincidentally aligned fractures, because these fractures could have either concordant or discordant propagation directions. The relative strength of bed contacts might provide further support for the interpretation of coincidental or stepped-over fractures. For example, fractures are not expected to propagate through or step-over at very weak bedding contacts.

The consistency of fracture intersection along a particular bedding contact could be used to confirm interpretation of coincidentally aligned fractures versus step-over fractures. If most of the long fractures within a thick layer are sub-aligned with fractures within an adjacent thinner layer, then a step-over mechanism is probable along the contact between the two layers. In contrast, occasional sub-alignment along a bed contact may indicate coincidental fracture alignment. In a similar fashion, the distance of step-over can be examined for consistency along any one bed contact that has consistent material properties and thickness. Since fracture length will not vary along beds of uniform thickness,

the distance between parent and daughter step-over fractures should be consistent with the length of fractures either in the thinner or thicker adjacent beds. Larger step-over distance is expected for fractures growing from the thicker layer (i.e. longer parent fracture), while smaller step-over is expected for fractures that propagate from the thinner layers. When the contact properties and bed thickness are consistent along a layer, a broad range of step-over distances is not expected.

6. Conclusions

The numerical experiments of this study explore the influence of deformation along bedding contacts, in the form of local sliding and/or debonding and subsequent opening, on fracture intersection with bed contacts. Fractures propagating toward a bedding contact may either (1) terminate at the contact, (2) propagate straight through the contact, or (3) step-over to the left or right at the bedding contact. The model results suggest that local interface opening, rather than sliding, is primarily responsible for the termination and step-over of fractures. Furthermore, the model results suggest that the strength of bedding contacts controls the type of resulting fracture intersection. Fracture termination is favored at very weak bedding contacts, whereas fractures propagate straight through strong contacts. Most sedimentary contacts will fall between these two end-members. Such moderate-strength contacts may develop step-over fractures due to local opening along the interface or, if the stresses are not great enough to produce new fractures, the parent fracture will terminate at the moderate-strength contact. Fracture termination is more likely under conditions of shallower burial depth, lower effective layer-parallel tension, and fluid-driven propagation, rather than equivalent remote layer-parallel tension. Thicker beds and greater effective layer-parallel tension may produce greater amounts of step-over than thinner beds and more compressive layers. Fractures aligned within several centimeters across a bed contact may be coincidentally aligned or the result of fracture step-over. Careful characterization of the fractures and analysis of the pattern may distinguish whether the fractures are the result of coincidental alignment or fracture step-over.

Acknowledgements

We thank Bill Dunne, Mike Gross, and Steve Martel for their thorough and extraordinarily helpful reviews of this manuscript. This work was partially supported by NSF grant EAR-9996296 to investigate bedding-plane slip mechanisms and by a Wisconsin Department of Natural Resources contract to investigate the mechanical controls on fracture development in carbonate aquifers. Discussions with Peggy Rijken, Toni Simo, Susan Murphy, and Maureen Muldoon helped develop the authors' ideas about bed contact deformation and/or improve this paper. Additionally, we appreciate the support of the Geological Engineering Program at UW—Madison.

References

Baer, G., 1991. Mechanisms of dike propagation in layered rocks and in massive porous sedimentary rocks. Journal of Geophysical Research 96, 11,911–11,929.

Bai, T., Gross, M.R., 1999. Theoretical analysis of cross-joint geometries and their classification. Journal of Geophysical Research, B, Solid Earth and Planets 104, 1163–1177.

Bai, T., Pollard, D.D., 2000. Fracture spacing in layered rocks; a new explanation based on the stress transition. Journal of Structural Geology 22, 43–57.

Becker, A., Gross, M., 1996. Mechanism for joint saturation in mechanically layered rocks: an example from southern Israel. Tectonophysics 257, 223–237.

Biot, M.A., Medlin, W.L., Masse, L., 1983. Fracture penetration through an interface. Society of Petroleum Engineers 23, 857–869.

Birch, F., 1966. Compressibility; elastic constants. In: Sydney, P., Clark, J. (Eds.). Handbook of Physical Constants, Memoir 97, Geological Society of America, pp. 97–173.

Broek, D., 1991. Elementary Engineering Fracture Mechanics. Kluwer Academic, Boston.

Budiansky, B., Hutchinson, J.W., 1986. Matrix fracture in fiber-reinforced ceramics. Journal of Mechanics, Physics and Solids 34, 167.

Byerlee, J., 1978. Friction of rocks. Pure and Applied Geophysics 116, 615–626.

Cook, T.S., Erdogan, F., 1972. Stresses in bonded materials with a crack perpendicular to the interface. International Journal of Engineering Science 10, 677–697.

Cooke, M., 1996. Frictional slip and fractures associated with faults and folds. Unpublished Ph.D. thesis, Stanford University.

Cooke, M., 1997. Fracture localization along faults with spatially varying friction. Journal of Geophysical Research 102, 22425–22434.

Cooke, M., Mollema, P., Pollard, D., Aydin, A., 2000. Interlayer slip and joint localization in East Kaibab Monocline, Utah: field evidence and results from numerical modeling. In: Cosgrove, J.W., Ameen, M.S. (Eds.). Geological Society of London Special Publication on Forced Folds and Associated Fractures 169, Geological Society, London, pp. 23–49.

Cooke, M., Pollard, D., 1997. Bedding plane slip in initial stages of fault-related folding. Journal of Structural Geology 19, 567–581.

Corbett, K., Friedman, M., Spang, J., 1987. Fracture development and mechanical stratigraphy of Austin chalk, Texas. AAPG Bulletin 71, 17–28.

Crouch, S.L., Starfield, A.M., 1990. Boundary Element Methods in Solid Mechanics. Unwin Hyman, Boston.

DeGraff, J.M., Aydin, A., 1987. Surface morphology of columnar joints and its significance to mechanics and direction of joint growth. Geological Society of America Bulletin 99, 605–617.

Delaney, P.T., Pollard, D.D., Ziony, J.I., McKee, E.H., 1986. Field relations between dike and joints: emplacement processes and paleostress analysis. Journal of Geophysical Research 91, 4920–4938.

Dyer, R., 1988. Using joint interactions to estimate paleostress ratios. Journal of Structural Geology 10, 685–699.

Erdogan, F., Biricikoglu, V., 1973. Two bonded half-planes with a crack going though the interface. International Journal of Engineering Science 11, 745–766.

Goodman, R.E., 1989. Introduction to Rock Mechanics. John Wiley, New York.

Gross, M., Fischer, M., Engelder, T., Greenfield, R., 1995. Factors controlling joint spacing in interbedded sedimentary rocks; integrating

numerical models with field observations from the Monterey Formation, USA. In: Ameen, M.S. (Ed.). Fractography. Geological Society Special Publication, Geological Society, London, pp. 215–233.

Gross, M.R., 1993. The origin and spacing of cross-joints: examples from the Monterey Formation, Santa Barbara, California. Journal of Structural Geology 15, 737–751.

Hanks, C., Lorenz, J., Teufel, L., Krumhardt, A., 1997. Lithologic and structural controls on natural fracture distribution and behavior within the Lisburne Group Northeastern Brooks Ranges and North Slope subsurface, Alaska. AAPG Bulletin 81, 1700–1720.

Helgeson, D.E., Aydin, A., 1991. Characteristics of joint propagation across layer interfaces in sedimentary rocks. Journal of Structural Geology 13, 897–991.

Hoagland, R.G., Hahn, G.T., Rosenfield, A.R., 1973. Influence of microstructure on fracture propagation in rock. Rock Mechanics 5, 77–106.

Hobbs, D.W., 1967. The formation of tension joints in sedimentary rock: an explanation. Geology Magazine 104, 550–556.

Huang, Q., Angelier, J., 1989. Fracture spacing and its relation to bed thickness. Geology Magazine 126, 355–362.

Jaeger, J.C., Cook, N.G.W., 1979. Fundamentals of rock mechanics. Science Paperbacks 18, 18.

Ji, S., Saruwatari, K., 1998. A revised model for the relationship between joint spacing and layer thickness. Journal of Structural Geology 20, 1495–1508.

Ji, S., Zhu, Z., Wang, Z., 1998. Relationship between joint spacing and bed thickness in sedimentary rocks: effects of interbed slip. Geology Magazine 135, 637–655.

Kulander, B.R., Barton, C.C., Dean, S.L., 1979. The application of fractography to core and outcrop fracture investigations. United States Department of Energy, Morgantown Energy Technology Center.

Lawn, B., 1993. Fracture of Brittle Solids. 2nd ed., Cambridge University Press, New York.

McQuillan, H., 1973. Small-scale fracture density in Asmani Formation Southwest Iran and its relation to bed thickness and structural setting. American Association of Petroleum Geologists Bulletin 57, 2367–2385.

Narr, W., Suppe, J., 1991. Joint spacing in sedimentary rocks. Journal of Structural Geology 13, 1037–1048.

Nelson, R.A., 1985. Geological Analysis of Naturally Fractured Reservoirs. Gulf, Houston, TX.

Nemat-Nasser, S., Keer, L.M., Parihar, K.S., 1978. Unstable growth of thermally induced interacting cracks in brittle solids. International Journal of Solids and Structures 14, 49–430.

Pollard, D.D., Aydin, A., 1988. Progress in understanding jointing over the past century. Geological Society of America Bulletin 100, 1181–1204.

Pollard, D.D., Segall, P., 1987. Theoretical displacements and stresses near fractures in rock, with application of faults, joints, veins, dikes and solution surfaces. In: Atkinson, B.K. (Ed.). Fracture Mechanics of Rock, Academic Press, London, pp. 277–349.

Price, N.J., 1966. Fault and Joint Development in Brittle and Semi-brittle Rock. Pergamon Press, Oxford.

Renshaw, C.E., Pollard, D.D., 1995. An experimentally verified criterion for propagation across unbonded frictional interfaces in brittle, linear elastic materials. International Journal of Rock Mechanics and Mining Science and Geomechanics Abstracts 32, 237–249.

Roering, J., Cooke, M., Pollard, D., 1997. Why blind thrust faults don't propagate to the earth's surface: numerical modeling of coseismic deformation associated with thrust-related anticlines. Journal of Geophysical Research 102, 11901–11912.

Suppe, J., 1985. Principles of Structural Geology. Prentice-Hall, Englewood Cliffs, NJ.

Tada, H., Paris, P.C., Irwin, G.R., 1985. The Stress Analysis of Cracks Handbook. Paris (& Del Research Coorporation), St. Louis.

Teufel, L.W., Clark, J.C., 1984. Hydraulic fracture propagation in layered rocks: experimental studies of fracture containment. Society of Petroleum Engineers Journal 24, 19–34.

Theircelin, M., Roegiers, J.C., Boone, T.J., Ingraffea, A.R., 1987. An investigation of the material parameters that govern the behavior of fractures approaching rock interfaces. 6th International Congress of Rock Mechanics, pp. 263–269.

Tsang, Y.W., 1984. The effect of tortuosity on fluid flow through a single fracture. Water Resources Research 20, 1209–1215.

Underwood, C.A., 1999. Stratigraphic controls on vertical fracture patterns within the Silurian dolomite of Door County, Wisconsin and implications for groundwater flow. Unpublished M.S. thesis, University of Wisconsin—Madison.

Weertman, J., 1980. The stopping of a rising, liquid-filled crack in the earth's crust by a freely slipping horizontal joint. Journal of Geophysical Research 85, 967–976.

Wu, H., Pollard, D.D., 1995. An experimental study of the relationship between joint spacing and layer thickness. Journal of Structural Geology 17, 887–905.